Appl. Phys. B 57, 249–259 (1993)

Applied Physics B Photophysics and Laser Chemistry



# A Model for Temperature-Dependent Collisional Quenching of NO $A^2\Sigma^+$

**P. H. Paul**[1], **J. A. Gray**[1], **J. L. Durant Jr.**[1], **J. W. Thoman Jr.**[2]

[1] Combustion Research Facility, Sandia National Laboratories, Livermore, CA 94550, USA
(Fax: +1-510/294-1004, e-mail: phpaul@ca.sandia.gov
[2] Chemistry Department, Williams College, Williamstown, MA 01267, USA

Received in revised form 13 July 1993/Accepted 3 August 1993

**Abstract.** A model for the temperature-dependent electronic quenching of NO $A^2\Sigma^+$ is presented. The model is appropriate for collision partners having stable negative ions, which are predicted to have large quenching cross-sections. Colliders with relatively large negative electron affinities are predicted to have cross-sections that are near-zero at room temperature and can increase dramatically at very high temperatures. A negligibly small electronic quenching cross-section is predicted for collision partners having negative ions that are unstable on a collisional timescale. Results of the model are compared to experimentally measured cross-sections for a number of species of interest in combustion and aerothermodynamic applications.

**PACS:** 34.10.+x, 34.30.+h, 82.20.Pm, 82.50.Et

Nitric oxide (NO) is an important combustion-generated pollutant as well as a key tracer species for laser-induced fluorescence flowfield diagnostics [1]. To use fluorescence techniques to study turbulence-chemistry interactions it is essential to be able to accurately correct the measured signal for variations in flowfield properties. Such corrections are practical for single point measurements since the requisite flowfield data can be measured by techniques such as laser Raman scattering [2]. For multipoint measurements it is not practical to gather the data needed for such corrections on a flow-stopping timescale. Thus to interpret a planar laser-induced fluorescence image as representing a particular flowfield property requires a model for fluorescence signal to properly select a suitable excitation /detection strategy.

A relation for the NO fluorescence signal can be developed by observing that: when the laser spectral energy flux is sufficiently low, a two-level steady-state approach describes the signal as long as rotational repopulation of the pumped state is reasonably fast [3]; the effects of multiple absorbing transitions are important owing to the relatively strong pressure broadening and dense rotational absorption spectrum exhibited by NO; and, the present experimental evidence suggests that the electronic quenching cross-section for NO is independent of rotational level [4–6]. In these limits and for broadband detection, the total fluorescence signal observed during the laser pulse is written as

$$S_{\mathrm{Lf}} = C_{\mathrm{opt}} E_p \sum_i [f_{Bi}(T) B_i g_i(\chi_p, P, T)] \times \{A/[A + Q(\chi_p, P, T)]\}\, \chi_{\mathrm{NO}} P/k_{\mathrm{B}} T\,, \quad (1)$$

where the summation is over all transitions $i$ which are pumped by the laser. Here $C_{\mathrm{opt}}$ is a collection of constants which describe the optical system, $E_p$ is the total laser energy per pulse, $A$ and $B_i$ are Einstein coefficients. The signal dependence on local thermodynamic conditions is through the Boltzmann population fraction, $f_{Bi}(T)$; the line shape function $g_i$ which is a convolution between the laser and absorption spectral profiles; the NO number density given by $\chi_{\mathrm{NO}} P/k_{\mathrm{B}} T$; and the electronic quenching rate given by $Q(\chi_p, P, T)$. Here $\chi_{\mathrm{NO}}$ is the NO mole fraction and the $\chi_{\mathrm{p}}$ are the mole fractions of the perturbing species. The total time-integrated signal must also include fluorescence that is collected after the laser pulse [e.g. $S_{\mathrm{f}} \approx S_{\mathrm{Lf}}(1+1/\tau_{\mathrm{L}}(A+Q))$, where $\tau_{\mathrm{L}}$ is the laser pulsewidth). Thus the measured signal has a complicated dependence on local temperature, pressure and the distribution of collision partners as well as a direct dependence on the number density of the absorbing species.

In recent years electronic quenching of NO $A^2\Sigma^+$ has come under increasing study [5–12]. Several general observations have been made from these data: the quenching cross-section for species having a positive electron affinity is of order gas-kinetic or greater and exhibits little or no temperature or rotational dependence; the cross-section for species with a negative electron affinity is quite small at room temperature but may rise dramatically with increasing temperature; at present there is no strong indication for rotational dependence; quenching by molecules having absorbing transitions at energies slightly lower than that of NO $A^2\Sigma^+$ may be exceptionally fast due to near-resonant dipole-dipole enhanced energy transfer; and finally, quenching proceeds with a disposition to produce vibrationally excited NO $X^2\Pi$ [13]. Any successful model for quenching

must predict all of the aspects of the experimental results including the variation with collision partner, the magnitude of the cross-section and the temperature dependence, and the diposition into final states.

A number of models that are based on long-range attractive forces have been used to predict the behavior of electronic quenching. None of these models appear to be consistent with the experimental observation for quenching of NO $A^2\Sigma^+$ [8]. Several of these models are correlations which predict an inverse power-law temperature dependence for all perturbing species and which cannot distinguish the very small cross-section measured for species such as $N_2$. A detailed collisional-complex model, based on multipole attractive forces and a centripetal barrier, has been successfully used to predict the quenching behavior of $SO_2$ $\tilde{A}^1A_2$ [14] and of OH $A^2\Sigma^+$ [15]. We have considered this latter model in some detail, even to the extent of including a rigorous thermal average over molecular orientations. We find reasonable performance in predicting the species and temperature-dependent behavior but not the magnitude for quenching of OH $A^2\Sigma^+$. However, this model appears to be inadequate to describe quenching of NO $A^2\Sigma^+$. Attractive force models require information about the electronic properties of the collision partners. Values of the excited state species are typically unknown and commonly taken to be near those of the ground-state. Greenblatt and Ravishankara [16] have suggested that the large cross-sections observed for quenching of NO $A^2\Sigma^+$ could be justified using a gas-kinetic diameter of 9.5 Å (a value obtained for NO $A^2\Sigma^+$ in a cryogenic matrix) or a polarizability of 85 Å$^3$ (a value obtained from an SCF simulation). Although changes to the molecular electronic properties in this fashion does increase predicted cross-sections, the net result remains an inverse-power temperature dependence and a large cross-section predicted for all collision partners.

Drake and Ratcliffe [6] have advanced two models for NO quenching: for strong quenchers, an empirical model based on a Parmenter-Seaver [17] well-depth correlation; and for weak quenchers, a model based on an activation barrier for transfer from the NO $A^2\Sigma^+$ state to the $a^4\Pi$, $b^4\Sigma$ or $B^2\Pi$ states. One consequence of invoking this form of intramolecular transfer to describe the quenching mechanism is a possible strong increase in the cross-section with increasing temperature as well as a strong rotational level dependence. Such a "gateway" mechanism, to the NO $a^4\Pi$ state (say), does not appear to be consistent with the present experimental data for quenching by $N_2$ [11].

A reasonably successful picture for NO quenching is one of electron transfer via an ion-pair intermediate formed between the excited state of NO and the collision partner [18]. At a basic level, this "harpoon" or "curve-crossing" model predicts a radius $r_c$ for transfer to the ion-pair surface that can be used to estimate a geometric cross-section (e.g., $\sigma_g = \pi r_c^2$). The value for this radius is largely determined by the value of the adiabatic electron affinity of the collision partner. To improve the predictive capability of this model, Asscher and Haas [18] and Haas and Greenblatt [19] have invoked the range of values between the vertical and adiabatic electron affinities as well as the possibility of a "reactive" affinity as a model variable, and they have further suggested a correction of the form $\sigma_\gamma = \pi r_c^2 \exp(-\gamma r_c)$. This latter correction may be seen as a correlation to the bond energy of the NO-M complex or to the overlap of the electronic wavefunction of the collision pair at the radius $r_c$. The constant was obtained by a best fit to 300 K experimental results to be $\gamma = 0.09$ when the ionic potential was taken to be simple Coulomb and $\gamma = 0.08$ when the ion polarizability was included [18]. While this correction does appear to improve this simple model in describing quenching of NO $D^2\Sigma^+$ it does not significantly improve the performance of the model as applied to NO $A^2\Sigma^+$.

For the harpoon model, a weak or temperature-independent cross-section behavior can be inferred from a theoretical development for the inverse reaction [20] (e.g. recombinative excitation, $Q^+ + M^- \Rightarrow Q^* + M$) and has been predicted for quenching of electronically excited sodium by $N_2$, $O_2$ and CO [21]. However, the same mechanism applied in the limit of weakly allowed electron transfer provides a cross-section with an inverse power-law temperature dependence [22]. In the following we consider the harpoon model in some detail to investigate the collision partner- and temperature-dependent behavior of quenching of NO $A^2\Sigma^+$. We first outline the assumptions used in the model, and we then consider the predicted asymptotic behavior of the thermally averaged quenching cross-section. Cross-section predictions are then compared to experimental values for a number of species of interest in combustion and aerothermodynamic applications.

## 1 Model Assumptions

The quenching rate is given by

$$Q = (P/k_B T)\langle v_{NO}\rangle \sum_p \chi_p (1 + m_{NO}/m_p)^{1/2} \langle\langle \sigma_p(T)\rangle\rangle \,, \quad (2)$$

where the summation is over all perturbing species, $p$, and $\langle v_{NO}\rangle \equiv (8k_B T/\pi m_{NO})^{1/2}$. The magnitude and temperature dependence of the thermally-averaged electronic quenching cross-section is perturbing species specific and defined by $\langle\langle \sigma_p\rangle\rangle = \langle v\sigma_p(v)\rangle / \langle v\rangle$. Here $\sigma_p(v)$ is the relative velocity dependent cross-section obtained by integrating the probability of quenching over the collision impact parameter, $b$. The thermal average is taken to be over a Boltzmann distribution of collision velocities. We invoke the conventional transformation, $\eta \equiv (v/\underline{v})^2$, where $\underline{v} \equiv (2k_B T/\mu)^{1/2}$, to obtain

$$\langle\langle \sigma_p\rangle\rangle = \pi \int_0^\infty \eta \exp(-\eta) \int_0^\infty P_{Q_p}(\eta \underline{v}^2, b^2) \mathrm{d}b^2 \mathrm{d}\eta \,. \quad (3)$$

Here $P_{Q_p}$ is the perturbing species specific probability for electronic quenching. To predict the thermally averaged cross-section we make the following assumptions:

1) In a collision, quenching is taken to occur by electron transfer from NO $A^2\Sigma^+$ to the collider, M, followed by ion-ion recombination to form an NO $X^2\Pi$–M covalent pair. The initial electron jump occurs at the intersection between the $NO_A$–M covalent and the $NO^+$–$M^-$ ionic surfaces (note: we introduce the subscripts to denote the NO neutral electronic states for notational simplicity). This ionic surface

in turn makes an inner crossing with the $NO_X$–M covalent surface on the repulsive wall. The crossings of the ionic surface with the $NO_A$–M and $NO_X$–M surfaces can then act as efficient entrance and exit channels for electronic quenching.

The crossings with the $NO_A$–M surface occur at radii $r_c$ which are determined from the solutions to $\varphi^{(i)}(r_c) = \varphi^{(c)}(r_c)$, where $\varphi^{(i)}$ and $\varphi^{(c)}$ are the ionic and covalent potentials, respectively. The multiple crossings correspond to sets of vibrational states in the neutrals and ions. The potentials are respectively taken to be given by

$$\varphi^{(c)}(r) = E_{NOA} + E_M + \varphi_c(r)\,, \tag{4a}$$

$$\varphi^{(i)}(r) = IP_{NOX} + E_{M^-} - E_{fM} - e^2/r - e^2 \times (\alpha_+ + \alpha_-)/2r^4 + \varphi_i(r)\,. \tag{4b}$$

Here $E_{NOA}$ is the energy of the NO $A$-state, $IP_{NOX}$ is the ionization potential for the NO ground-state, $E_{fM}$ is the adiabatic electron affinity of the quencher, and $\alpha$ is a molecular polarizability. $E_M$ and $E_{M^-}$ are the energies of the vibrational state of the collision partner and its respective ion.The vertical electron affinity is defined by $E_{vM} = E_{fM} - E_{M^-}$. The potentials $\varphi_c(r)$ and $\varphi_i(r)$ are taken to be long-range attractive multipoles (the balance of the multipole terms for the case of the ion) combined with short-range repulsive terms.

As point multipoles, the long-range portions of these potentials contain orientation dependent terms. The difference in the multipole terms [23] may be written as

$$\varphi^{(i)} - \varphi^{(c)} \propto e^2 \sum_{n\geq 1} C''_n/r^n + e \sum_{n\geq 2} C'_n/r^n + \sum_{n\geq 3} C_n/r^n\,. \tag{4c}$$

The lead series is usually dominant due to strong charge-charge interactions and is angle independent. The latter two series present a complicated dependence on relative molecular orientation but the coefficients are relatively small and in the last series they appear as differences between those for the ion and covalent pairs. In the present simulation the attractive terms in $\varphi_c$ and $\varphi_i$ are modeled as thermally orientation-averaged multipoles [24, 25] while the repulsive terms are taken in the form of Buckingham exponentials [i.e. $\varphi_{rep}(r) = A\exp(-rB)$].

2) The collision may be considered as a cycle of approach and separation. In a collision that reaches $r_c$ let $P_Z$ be the probability of remaining on $NO_A$–M surface (that is a crossing, not transferring an electron). One convention has been to assume that the quenching probability is equal to that for remaining on the ionic surface after one cycle [26], giving $P_Q = 2P_Z(1 - P_Z)$. An alternative has been to take the quenching probability as equal to that for transfer to the ionic surface on the initial approach [18], giving $P_Q = 1 - P_Z$. We take an alternate approach. At the end of the first cycle, some fractions of the flux incident on a particular $NO_A$–M surface will be elastically reflected along that surface, some fraction will be quenched to exit along the $NO_X$–M surfaces with the balance remaining on the ionic surfaces. This latter fraction will recycle through the process a number of times to finally exit along some $NO_A$–M or $NO_X$–M surface. Let $(1 - P_R)$ be the probability of electron transfer in an interaction with the $NO_X$–M surface, then the infinite sum for this process gives

$$P_Q = (1 - P_R)(1 - P_Z)/[1 - P_Z(1 + P_R)/2]\,. \tag{5}$$

In the limit that there is no transfer to the $NO_X$–M surfaces ($P_R = 1$) this gives $P_Q = 0$ independent of the value of $P_Z$. For the case of complete exit channel transfer ($P_R = 0$) the probability of quenching becomes $P_Q = (1 - P_Z)/(1 - P_Z/2)$.

In actuality, the interaction between the excited covalent and ionic surfaces is more properly characterized by a complex grid of crossings which correspond to the positive and negative ion vibrational states accessible in the collision [18, 21, 27, 28]. The probability for electron transfer depends strongly on the degree of neutral-ion vibrational overlap in both electron donor and acceptor. Since NO $A^2\Sigma^+$ is a Rydberg state, the primary electron transfer channels will be for the $\Delta v = 0$ crossings of $NO_A \leftrightarrow NO^+$. Thus the probability of remaining on the covalent surface upon approach is given by $P = \prod_i P_i$, where the product runs over the set of crossing defined by the energetically accessible vibrational states of the negative ion. Again three trajectories through this grid are possible: 1) electron transfer does not occur on approach or on separation, the result being elastic scattering which occurs with a probability of $P^2$; 2) electron transfer occurs on approach resulting in quenching with a probability of $1 - P$; 3) electron transfer occurs upon separation with a probability of $P(1-P)$, at low energies the result is a subsequent cycle while at heigh energies there is a possibility for vibrational energy transfer (e.g. separation with vibrational excitation or de-excitation of the $NO_A$ or of the collision partner). The probability for electronic quenching then has an upper bound of $P_Q = 1 - P^2$ at low temperature and a lower bound $P_Q = 1 - P$ at high temperature. In our model we consider the full grid of entrance channels and adopt a "unit-flux" algorithm to calculate the total quenching probability.

3) The interaction between the ionic $NO_X$–M covalent surfaces in a far more complex grid of crossings owing to the accessibility of a large number of vibrational channels for $NO^+ \leftrightarrow NO_X$ and for $M^- \leftrightarrow M$. A significant number of these crossings lie deep within the ionic well, which suggests that the total probability for ionic to ground-state transfer should be weakly dependent on initial kinetic energy. Further, a fraction of the flux returned towards the $NO_A$–M surface will be in excited states of the positive ion. Recycling of vibrationally excited states of $NO^+$ is highly favored since the corresponding exit channels must be for vibrationally excited states of $NO_A$ which may not even be accessible from an energetic standpoint. We assume that the probability of transfer from the ionic to the $NO_X$–M surface is suitably large and insensitive to the relative kinetic energy of the collision, hence $P_R$ is taken to be a constant for any given collision partner and thus is a free parameter of the solution.

4) At $r_c$ the probability of remaining on the $NO_A$–M or $NO^+$–$M^-$ surface is taken to be that given by the Landau-Zener theory [26], $P_Z(w_{LZ}) = \exp(-w_{LZ})$, where

$$W_{LZ} = 4\pi^2 H'^2_{12}(r_c)/h v_{rad} \Delta\varphi'(r_c)\,. \tag{6}$$

Here $v_{\rm rad}$ is a radial velocity and

$$\Delta\varphi'(r_{\rm c}) = |\partial[\varphi^{(\rm c)}(r) - \varphi^{(\rm i)}(r)]/\partial r|_{r_{\rm c}} . \quad (7)$$

$H'_{12}$ is the matrix element of the perturbation potential which mixes the zero'th order states, and is taken to be non-negligible only in the neighborhood of $r_{\rm c}$. For molecular collision partners the matrix element can be approximated as a product of an electronic term and a vibrational overlap factor, $H'^2_{12} = h'^2_{12}|\langle {\rm NO}_A|{\rm NO}^+\rangle|^2|\langle {\rm M}|{\rm M}^-\rangle|^2$. Here the latter two terms are the donor and acceptor Franck-Condon factors, respectively.

The matrix element is also formally dependent on molecular orientation. The effect of including orientation as a separable term in the definition of $h'_{12}$ has been considered by Gislason and Sachs [27]. For example, taking $W = w\cos^2\theta$ the average of $P_Z(W)$ over all angle gives $P_Z(w) = \sqrt{(\pi/4w)}{\rm erf}(\sqrt{w})$, while a $\sin^2\theta$ dependence provides a functionally similar result in terms of the incomplete gamma function. In the present formulation of the model we assume that there is a weak dependence on orientation which would be appropriate in the limit that the molecules rotate sufficiently fast to equally sample all possible orientations or if the angular dependence is sufficiently "lobed" so as to appear isotropic given some small degree of rotational blurring. When compared to the isotropic dependence, asymptotic solutions for a $\cos^2\theta$ or $\sin^2\theta$ dependence show a decrease in the predicted quenching cross-section but show a functionally similar temperature dependence.

5) The outer-most crossing takes place at a relatively large radius, thus the electronic interaction results from an overlap of the tails of the electronic wave-functions and can be modeled via the Hasted-Chong correlation [29] here taken to be in the parametric form proposed by Olsen et al. [30].

$$h'^2_{12} = IP_{\rm NO}A E_{\rm fM}/I_{\rm H}(r_{\rm c}/2a_0)^2(\sqrt{IP_{\rm NO}A} + \sqrt{E_{\rm fM}})^2 \times \exp[-C(r_{\rm c}/a_0)(\sqrt{IP_{\rm NO}A} + \sqrt{E_{\rm fM}})/\sqrt{I_{\rm H}}], \quad (8)$$

where $I_{\rm H}$ is the ionization potential for hydrogen and $a_0$ is the Bohr radius. The constant is taken as $C = 0.86$, which is a best fit to a large set of charge transfer and ion-ion recombination reaction date [30]. Predicted values should be reasonably accurate to within a factor of two, but are likely to be biased low [27]. It is important to note that this correlation is defined in terms of the adiabatic affinity and $r_{\rm c}$, whereas $r_{\rm c}$ is functionally dependent on the vertical affinity.

6) The collision is modeled with a straight-line trajectory. This gives

$$v_{\rm rad} = \{v^2(1 - b^2/r_{\rm c}^2) + 2[\varphi^{(\rm c)}(\infty) - \varphi^{(\rm c)}(r_{\rm c})]/\mu\}^{1/2} , \quad (9)$$

where $b$ is the collision impact parameter. We take the probability for electron transfer at a crossing to be finite for $b \le r_{\rm c}$ and identically zero for $b > r_{\rm c}$.

The NO $A^2\Sigma^+$ state should exhibit a relatively large dipole moment and polarizability. This could make the covalent surface strongly attractive leading to the formation of centripetal barrier. Such long-range attractive characteristics can significantly affect the cross-section prediction. Various formalisms for implementing a centripetal barrier in a collision calculation are reviewed by Su and Bowers [31]. We employ a somewhat different approach that expedites the calculation: the attractive part of the covalent potential is taken to be a multipole given by $\Psi_0 = -\Sigma r^{-n}C_n/k_{\rm B}T$. We then define a set of functions $\Psi_j \equiv -r^2\partial\Psi_{j-1}/\partial r^2$. The location and the energy of this barrier are determined by finding the impact parameter and radius pairs, $(b^*, r^*)$, which satisfy

$$\eta b^{*2} = r^{*2}\Psi_1(r^*) \quad \text{and} \quad \eta = \Psi_1(r^*) - \Psi_0(r^*) . \quad (10)$$

Equations (10) are a transcendental pair, but the argument of the velocity integral can be made explicit by an analytical transformation to a radial metric. When $b^* > r_{\rm c}$ the cross-section is obtained by integrating a velocity-dependent capture cross-section given by $\sigma(v) = \pi b^{*2}$. For $b^* < r_{\rm c}$, $\sigma(v)$ is obtained by integrating the probability of quenching via the ion-pair intermediate over impact parameter.

The formalism described above is termed the "full" model: that is, a simulation including the entire excited-state acceptor-donor grid and the action of a collision complex. This may be directly applied to atomic and diatomic collision partners. For polyatomic quenchers, we limit the use of the full model to a single outer crossing combined with a collision-complex unless the acceptor Franck-Condon array is available. The predictions reported in Gray et al. [10] made use of a much more limited formulation; a single outer-crossing harpoon model with Lenard-Jones attractive potentials. The predictions reported in Thoman et al. [11, 12] were made using the full model as stated here. We now consider the asymptotic behavior of the model as applied to quenching of NO $A^2\Sigma^+$.

## 2 Asymptotic Trends in the Quenching Cross-Section

The harpoon process is parameterized by three characteristic velocities: the most probable thermal velocity, $\underline{v}$; a velocity associated with the change in kinetic energy in reaching the outer crossing, $v_E \equiv \{2[\varphi^{(\rm c)}(\infty) - \varphi^{(\rm c)}(r_{\rm c})]/\mu\}^{1/2}$, and $v_{LZ} \equiv w_{LZ}v_{\rm rad}$. For a crossing on the attractive portion of the potential, these appear in two non-dimensional groups, $\Gamma \equiv (\underline{v}/v_{LZ})^2$ and $D/\Gamma = |\varphi_{\rm c}(r_{\rm c})|/k_{\rm B}T$. This latter group is expected to be small for most cases of interest here. For pure harpoon quenching the thermally averaged cross-section is then given by

$$\langle\langle\sigma\rangle\rangle = \pi r_{\rm c}^2 \int_0^\infty \eta\exp(-\eta)\int_0^1 P_Q(w_{LZ}){\rm d}s{\rm d}\eta , \quad (11)$$

where $w_{LZ} \equiv (\Gamma\eta s + D)^{-1/2}$ and $s \equiv 1 - b^2r_{\rm c}^2$.

The character of the solution can be illustrated by first considering the case of a single outer crossing. Excluding the case of $P_R = 1$, (5) can be expanded in an infinite series in powers of $P_Z$. Within the series, the individual integrals of $P_Z^n(w_{LZ})$ over impact parameter can be performed analytically, thus integrating by parts and resuming the series under the velocity integral we find

$$\langle\langle\sigma\rangle\rangle = \pi r_{\rm c}^2(1 - P_R)\left[1 - \frac{(1 - P_R)}{2}\exp(D/\Gamma) \times \int_{D/\Gamma}^\infty \frac{\exp(-\eta){\rm d}\eta}{\exp(1\sqrt{\Gamma\eta}) - (1 + P_R)/2}\right] . \quad (12)$$

For small values of $\Gamma$, that is for $v_{LZ} \gg \underline{v}$, the asymptotic solution is given by $\langle\langle\sigma\rangle\rangle \propto \pi r_c^2(1 - P_R)$ which is independent of temperature. For values of $\Gamma$ of order unity the numerical solution is found to vary quite slowly with temperature.

We now consider the case of a grid of acceptor crossings. The total probability of transfer to the ionic surfaces as the particles approach is given by $P_Q = 1 - P_Z(-\Sigma w_i)$, where the summation runs over the set of crossings defined by the energetically accessible vibrational states of the negative ion. We have performed a parametric study of NO $A^2\Sigma^+$ quenching by a prototype diatomic molecule as a function of the adiabatic electron affinity. This prototype molecule was taken to be the same as NO $X^2\Pi$, but with the adiabatic affinity as a free variable. The Franck-Condon array for the donor was taken as purely diagonal. The acceptor array was obtained from a "reflection" approximation for bound-bound transitions [32] with the (0,0) value taken from NO photodetachment measurements [33]. Other properties required for the simulation are listed in Table 1. We found little or no temperature dependence for $0 < E_{fM} = 1.0$ eV. This result is apparently driven by a small value of $\underline{v}/v_{LZ}$ at the outer-most crossing. For avalue of $E_{fm} = 1.5$ eV we found that the cross-section varies as $T^{-0.1}$ for low temperatures, becoming nearly constant for $T > 900$ K. When the value for $r_c$ is driven by a moderately positive affinity and the ground-state acceptor Franck-Condon factor is of order one-tenth, the cross-section is found to be functionally constant with temperature. However, a large positive affinity leads to a low value for the electronic matrix element at the outer-most crossing, such crossings are then less effective at quenching with increasing velocity hence increasing temperature.

Crossings which occur at a very large radius will result in a small value for $h'_{12}(r_c)$. This combined with a vanishingly small value for the acceptor Franck-Condon element would result in a low value for $v_{LZ}$. In the limit of $v_E \gg v_{LZ}$, (11) can be integrated analytically to yield

$$\langle\langle\sigma\rangle\rangle = (1 - P_R)(2\pi^{3/2} r_c^2/\sqrt{\Gamma}) \times \exp(D/\Gamma)\mathrm{erfc}(\sqrt{D/\Gamma}\,. \tag{13}$$

This result gives the thermally-averaged cross-section falling with increasing temperature, roughly as $\langle\langle\sigma\rangle\rangle \propto T^{-0.9}$. This is similar to the conventional result obtained by assuming that quenching is given by the probability of remaining on the ionic surfaces in the first cycle and in the limit that $w_{LZ}$ is small over the entire range of the velocity integral [22].

A full simulation for polyatomic molecules is quite involved. However, a general trend can be inferred from the model. At some impact parameter $b_o < r_c$ the large number of crossings, each with a small but finite probability for electron transfer, will sum to give an effectively large value for $v_{LZ}$ and thus a temperature independent contribution to the total cross-section of $\sigma_0 = \pi b_0^2$. At low temperatures, crossings at larger radius will be effective owing to the low radial velocity, the cross-section would then be given by $\sigma_g = \pi r_c^2$ and should decay with increasing temperature to a limiting value of $\sigma_0$. This decay should follow the asymptotic result given by (13). This type of behavior is expected

**Table 1.** Molecular constants used in the model

| | $\alpha$ [b] [Å$^3$] | $\alpha$ [Å$^3$] | $\mu$ [b] [D] | $q$ [b] [DÅ] | $I_p$ [b] [eV] | $E_{fM}$ [eV] |
|---|---|---|---|---|---|---|
| NO($X$) | 1.74 | 2.7 [m] | 0.1578 [c] | −2.4 | 9.25 | 0.026(±0.005) [f] |
| NO($A$) | 2.7 [m] | | 1.1 [j] | 1.8 | | |
| $NO^+$ | 0.7 [m] | | 0.1 [m] | 0.79 [h] | 30.3 | |
| $H_2O$ | 1.45 | 20.0 [a] | 1.8473 | 0.13 | 12.614 | −0.5 [a] |
| $CO_2$ | 2.65 | 30.0 [a] | 0.0 | −4.3 | 13.79 | −0.2 [a] |
| $NO_2$ | 3.0 | 40.0 [a] | 0.32 | | 9.78 | $2.3 < E_{fM} < 2.5$ [d] |
| $N_2O$ | 3.0 | 30.0 [m] | 0.1608 | −3.0 | 12.89 | 0.24 [d] |
| $O_2$ | 1.59 | 2.6 [m] | 0.0 | −0.39 | 12.071 | 0.451(0.007) [f] |
| CO | 1.95 | 8.0 [a] | 0.1098 | −2.5 | 14.014 | −1.375 [g] |
| Ar | 1.642 | | | | 15.76 | u |
| He | 0.205 | | | | 24.586 | u |
| $N_2$ | 1.75 | 8.2 [a] | 0.0 | −1.52 | 15.581 | −1.925 [e] |
| $H_2$ | 0.803 | 20.0 [m] | 0.0 | 0.651 | 15.4259 | $-2.4 < E_{fM} < -3$ [d], u |
| $NH_3$ | 2.22 | 3.22 [m] | 1.47 | −1.0 | 10.15 | 0.38 [d] |
| $CH_4$ | 2.56 | 3.65 [m] | $5.4 \times 10^{-6}$ | 0.0 | 12.98 | u |
| CH | 0.56 [n] | 1.65 [m] | 1.45 | | 10.64 | 1.24 [d] |
| OH | 0.98 [n] | 1.8 [m] | 1.655 [o] | 1.8 [k,o] | 12.9 | 1.8277 [d] |
| O | 0.8 | 5.94 | | | 13.618 | 1.463 [d] |
| H | 0.667 | 33.4 | | | 13.599 | 0.75421 [d] |
| NH | 0.75 [n] | 1.75 [m] | 1.3–1.7 | −0.3 | 13.1 | 0.381(±0.014) [d] |
| $SO_2$ | 3.8 | 20.0 [m] | 1.633 | 4.4 | 12.34 | 1.06 [d] |
| $SF_6$ | 6.55 | 35.0 [a] | 0.0 | 0.0 | 15.7 | 0.54(+0.1, −0.17) |

[a] Selected as fit to data within expected range, see text
[b] [35]. Values quoted for the vibrational ground state
[c] $\mu(NO_x, v' = 1) = 0.1416$ D, [36]
[d] [20, 52]
[e] [37]
[f] [33]
[g] Inferred from: [55]
[h] [36]
[j] [47, 48]
[k] [56]
[m] Assumed value
[n] Estimated from bond polarizabilities [24] and from [53]
[o] For $OH^-$, $\mu = 3.2$ D and $q = 2.5$ DÅ, [54]
[u] Highly unstable negative ion

for quenching by polyatomics with large electron affinities (e.g. $NO_2$ and a number of halocarbons). From a simple geometric argument, we expect that the value for $b_0$ should be larger than $b_Z \equiv \sqrt{2r_{LZ}}$, where $r_{LZ}$ is the radius that gives a maximum in $v_{LZ}$. Collision partners which exhibit a large electron affinity should have an ion polarizability not significantly greater than that for the neutral. Thus taking the ionic potential to be simple Coulomb gives, $r_{LZ} = (4a_0/C)\sqrt{I_H}/(\sqrt{IP_{NO,A}} + \sqrt{E_{fM}})$.

Quenching by a particular species cannot be distinguished purely on the basis of electron affinity. The negative ion polarizability, neutral-ion vibrational overlap, and character of the long-range potential of the collision pair play equivalently important roles. We now turn to specific predictions of the model. For atomic and diatomic collision partners we employ the "full" model. For triatomic colliders we employ a single-outer-crossing harpoon model combined with a collision-complex. For more complex polyatomic colliders we investigate the limiting case predictions of the harpoon model alone.

## 3 Model Results

Harpoon quenching is not prohibited for colliders with negative electron affinities as long as the negative ion is sufficiently stable. The affinity of $H_2$ is nearly $-3$ eV, which is comparable to the autodetachment width of the negative ion, $H_2^{-2}\Sigma_u^+$. The large negative value for the affinity as well as the very short lifetime of the ion suggest a negligibly small cross-section for quenching by $H_2$ at thermal energies. The same behavior would be expected for the nobel gases, $CF_4$, $SiF_4$ and many of the fully saturated hydrocarbons; that is, the entrance channel for electron transfer is energetically inaccessible and the negative ion is unstable towards autodetachment on the collisional timescale. This prediction appears to be well confirmed by experimental measurements (see Table 2). Many of these measurements (Table 2) are considered as upper bounds for quenching by these species, presumably owing to the presence of trace contaminants (e.g. water and $O_2$).

The negative ions of $N_2$, CO, $H_2O$, $CO_2$ and excited vibrational levels of $NO_X$ are sufficiently stable to have been experimentally studied in some detail (e.g. the lifetime for $CO_2^-$ is of order 60 μs). Since the added electrons in $N_2^-$ and $CO^-$ are in weakly bound orbitals, the polarizability of these ions could be quite large (for $N_2^-$, a value of $\alpha_- = 14$ Å$^3$ gave reasonable agreement with experimental results for quenching of electronically excited Na [21] and a value as high as 40 Å$^3$ has been suggested [28]). For such large values of the polarizability, the $r^{-4}$ term in the ionic potential becomes very significant, even to the extent that a moderately negative electron affinity can still yield a relatively large crossing radius. For such large ion polarizabilities, we include the contribution of the hyperpolarizability, an attractive sixth-order term in the ionic potential with the coefficient, $C_{ei-Q} = -e^2\alpha_Q/2$. Here $\alpha_Q$ is the quadrupole polarizability which was estimated from a harmonic oscillator model [34] to be $\alpha_Q \approx 3/2(\alpha_{NO^+}^2 IP_{NO^+} + \alpha_-^2 IP_{M^-})/e^2$.

The electron affinities of $N_2$ and CO have been measured to be $-1.925$ eV and $-1.375$ eV, respectively (see Table 1). These values are sufficiently negative to present an energy barrier to the harpoon mechanism since $r_c$ is on the repulsive wall of the $NO_A$–M surface. When a simple barrier with energy $\varepsilon_p$ is present, the cross-section is given by

$$\langle\langle\sigma(T)\rangle\rangle = \langle\langle\sigma(T_\infty)\rangle\rangle \exp(-\varepsilon_p/k_B T)\,. \tag{14}$$

In this limit, the high temperature cross-section is given by $\langle\langle\sigma(T_\infty)\rangle\rangle = \pi r_c^2$ and the height of the energy barrier is $\varepsilon_p = \varphi^{(c)}(r_c) - \varphi^{(c)}(\infty)$.

To test the sensitivity to the choice of parameters, simulations were run for a range of negative ion polarizabilities and covalent repulsive potentials. Coefficients for the repulsive potentials, required for the $N_2$ and CO quenching calculations, are taken from Mason and McDaniel [34] and Radzig and Smirnov [35], for the ion and covalent pairs, respectively. The acceptor Franck-Condon array for $N_2$ was taken as identical to that for the NO $\gamma$ system. Spectroscopic parameters were taken from Huber and Herzberg [36] for the neutrals and $NO^+ X^1\Sigma^+$, and from Lofthus and Krupenic [37] for $N_2^- X^2\Pi_g$. Other parameters required for the simulation are given in Table 1. For quenching of $NO\,A^2\Sigma^+$ ($v' = 0$) by $N_2$ we find outercrossing radii and energy barriers at 300 K to be (2.72 Å, 2080 cm$^{-1}$) and (3.307 Å, 275 cm$^{-1}$) using an NO–$N_2$ covalent repulsive potential and negative ion polarizabilities of 5 Å$^3$ and 15 Å$^3$, respectively. Using an NO–NO covalent repulsive potential, these values change to (2.76 Å, 2172 cm$^{-1}$) and (3.311 Å, 359 cm$^{-1}$), respectively. The most noticeable effect of varying the ion

**Table 2.** Measured cross-sections (Å$^2$) for species with unstable negative ions

| He | Ne | Ar | $CH_4$ | $CF_4$ | $H_2$ | $C_2H_6$ | $T$ [K] | Ref. |
|---|---|---|---|---|---|---|---|---|
| | | 0.006 | | | 0.0019 | 0.023 | 300 | [6] |
| | | | | | 0.0078 | | 793 | |
| | | | | | | 0.037 | 813 | |
| | | 0.002 | | | | | 995 | |
| <0.005 | | <0.015 | | | | | 1848 | [10] |
| | | 0.0033 | <0.001 | | | | 300 | [12] |
| | | 0.01 | <0.1 | | | | 1450 | |
| | | 0.01 | | | <0.22 | | 1880 | |
| | | | | | <0.52 | | 2307 | |
| | <0.017 | <0.007 | | <0.084 | <0.004 | | 300 | [16] |
| | | | <0.01 | <0.04 | <0.1 | | 300 | [19] |
| 0.002 | | 0.005 | | | 0.003 | | 300 | [39] |
| | | | 0.4 | | | | 300 | [43] |

polarizability or the character of the covalent repulsive potential is to change the level of the energy barrier. However, small changes to the radius and the curvature of the potentials at $r_c$ can significantly influence the value for $h'_{12}$, hence the crossing probability.

For predictions of quenching by $N_2$ we employ the NO–$N_2$ covalent repulsive potential and take values of $\alpha_- = 8.2$ Å$^3$ and $P_R = 0.55$, which provides a reasonable match to the measured cross-section at 300 K and to the energy barrier inferred from several low-temperature measurements. Figure 1 shows the predicted cross-section as a function of temperature, for quenching by $N_2$ in the vibrational ground-state and for a set of crossings weighted by the Boltzmann distribution for vibrational states of the collision partner. Consideration of the vibrational energy distribution of the collision partners provides a noticeable increase in the cross-section at higher temperatures. This results from an increase in the crossing radius and a decrease in the apparent energy barrier with increasing thermal vibrational excitation of the $N_2$. Also shown in Fig. 1 are several sets of measured cross-sections. The predictions follow the low temperature behavior of the measurements quite well. In the intermediate temperature range the predictions rise much more slowly than the data of Drake and Ratcliffe [6] while following the data of Thoman et al. [11]. The model underpredicts the measured trend at high temperatures; this may be the result of systematic errors in the measurement, may indicate the onset of a second quenching mechnism, or may be the consequence of assuming constant molecular electronic properties with increasing vibrational level in the model.

For quenching of excited vibrational levels of NO $A^2\Sigma^+$ by $N_2$ at 300 K; Imajo et al. [38] reported values of 0.012, 0.23 and 0.12 Å$^2$ for $v' = 0$, 1 and 2, respectively; Asscher and Haas [18] reported values of 0.01 and $< 0.01$ Å$^2$ for $v' = 1$ and 3, respectively; while other measurements [5, 39] give values of 0.014, 0.076 and 0.137 Å$^2$ for $v' = 0$, 1 and 2, respectively. The trend is an increase in the cross-section with increasing vibrational level in $NO_A$. This would not be expected from the model for a perfectly diagonal electron donor Franck-Condon array. When compared to the diagonal crossing, the non-diagonal crossing $\langle NO_A(v' = 1)|NO^+(v'' = 0)\rangle$ presents a lower energy barrier as well as occurring at a larger radius and on a more weakly sloped portion of the covalent potential. These latter two factors increase the value of $h'_{12}$ which offsets some of the effect of the poor vibrational overlap. The result of including the non-diagonal terms of the electron donor is a prediction of a factor of 2.4 times increase in the cross-section for quenching of $NO_A(v' = 1)$ over that for $NO_A(v' = 0)$ by $N_2$ at 300 K. This is predicted to drop to a value of 1.7 times at 2000 K which is somewhat lower than the observations of Thoman et al. [11] who reported cross-sections of 0.67 Å$^2$ and 2.2 Å$^2$ at 1900 K for $v' = 0$ and 1, respectively.

Figure 2 shows the results of the full model (with $P_R = 0$) and experimental data for quenching by CO. The values used for the simulation are given in Table 1. The vibrational structure of $CO^- X^2\Pi$ is assumed to be identical to that for $N_2^- X^2\Pi_g$ except that it is reduced by the ratio of the first vibrational spacing of the neutrals. The acceptor Franck-Condon array for CO was taken as identical to that for the CO Cameron system [21]. The present model is not capable of reproducing the low-temperature cross-section of 6 Å$^2$ measured for quenching by CO. However, the model result appears quite reasonable when added to a constant cross-section of 5.5 Å$^2$. One possible explanation for the low temperature behavior is near-resonant $E \rightarrow V$ transfer which would operate for CO (owing to a dipole moment of 0.1 D) but not for $N_2$ or $H_2$. Such a process has been observed for electronic quenching of electronically excited oxygen by CO [40] (e.g. $O(^1D) + CO(v = 0) \rightarrow O(^3P) + CO(v) + \Delta E$) and by mercury [41]. Using the several prodecures outlined by Breckenridge et al. [42] we estimate a cross-section of 3.7 Å$^2$ for near-resonant $E \rightarrow V$ quenching by CO at 300 K. One would expect that this will fall with increasing temperature, functionally between $\sigma \propto T^{-1}$ and $\ln\sigma \propto T^{-1/3}$. The action of the combined harpoon and $E \rightarrow V$

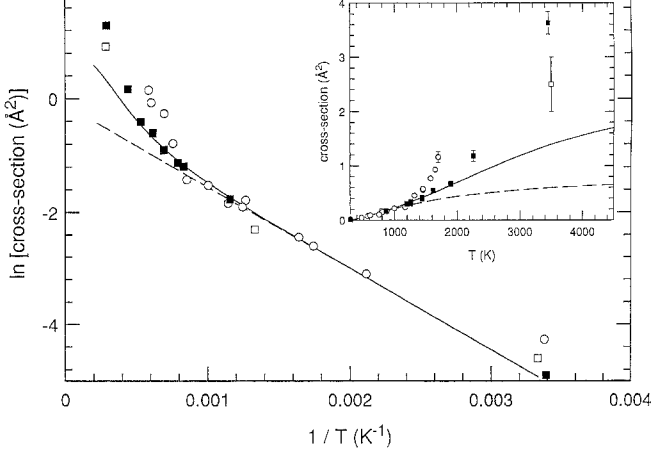


**Fig. 1.** Cross-section for quenching of NO $A^2\Sigma^+$ ($v' = 0$) by $N_2$ shown as an Arrhenius plot. *Dashed line*: prediction for collisions with ground state $N_2$. *Solid line*: prediction for collisions with a thermal distribution of $N_2$ vibrational states. Measured values: ■ [11], □ [6], ○ [8, 9]. The inset figure shows the same predictions and measured data plotted in linear form

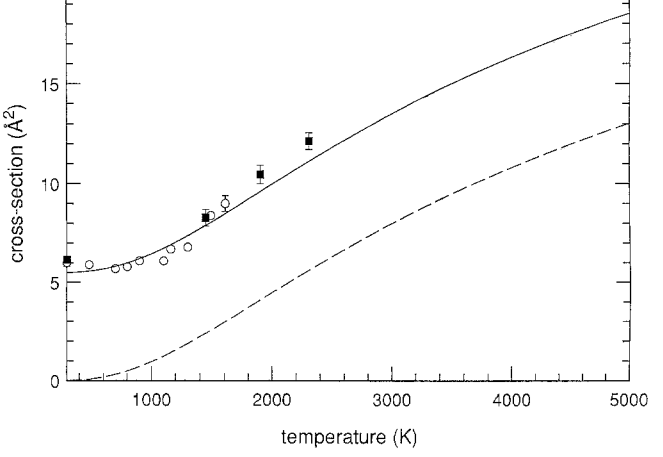


**Fig. 2.** Cross-section for quenching of NO $A^2\Sigma^+$ ($v' = 0$) by CO. *Dashed line*: predicted for collisions with a thermal distribution of CO vibrational states. *Solid line*: prediction added to an arbitrary constant cross-section of 5.5 Å$^2$ (see text). Measured values: ■ [12], ○ [6]

mechanisms is consistent with the experimental observations at low and intermediate temperatures. The behavior seen in quenching by CO is an example of the action of a secondary quenching mechanism which operates in parallel with harpoon quenching but which is only apparent when the harpoon process is poorly allowed. Presumably, as with quenching by $N_2$, the model will underpredict the CO quenching cross-section at extremely high temperatures.

The results of the full simulation and several sets of measured cross-sections for quenching by NO and $O_2$ are shown in Fig. 3. Here again, the acceptor Franck-Condon arrays were obtained from a "reflection" approximation for bound-bound transitions [32] with the (0,0) values and the negative ion spectroscopic factors taken from photodetachment measurements [33]. Values of $P_R = 0.07$ and 0.56 for NO and $O_2$, respectively, were found to provide a suitable match to the experimental data (note that in the model, $1 - P_R$ is a simple multiplicative constant in the value of the predicted cross-section). In both cases nearly temperature-independent behavior in the cross-section is predicted. The difference between the slight increase in cross-section with temperature predicted for quenching by NO and the slight decrease predicted for $O_2$ appears to be driven by the differences in the acceptor Franck-Condon arrays and the vibrational energies of the neutrals. Here we have included non-diagonal donor channels in the simulation, but their effect is imperceptible compared to the action of the diagonal terms. Since the vibrational frequencies in NO $A^2\Sigma^+$ and $NO^+$ $X^1\Sigma^+$ are nearly identical, quenching by NO and $O_2$ is predicted to be very weakly dependent on the vibrational level in NO $A^2\Sigma^+$. For quenching by NO and $O_2$ there is evidence to confirm this behavior in the results of Asscher and Haas [18] and Haas and Asscher [43], while Imajo et al. [38] reported NO self-quenching cross-sections of 35, 32 and 27 Å for $v' = 0$, 1 and 2, respectively.

In combustion systems, both $CO_2$ and $H_2O$ are important quenching partners. These molecules display large NO quenching cross-sections that fall rapidly with increasing temperature. Both of these species display moderately negative affinities. Reported values for the affinity of $CO_2$ range from +3.8 eV [44] to an estimate of +1 eV [45] to measured and calculated values in the range of −0.1 eV to −1 eV [46]. Similarly, for water, values range from +0.9 eV [44] to −0.8 eV [45]. Using the parameters in Table 1 and ion polarizabilities equal to those of the neutral molecules, we find the crossing radii are 3.4 Å and 3.7 Å for $H_2O$ and $CO_2$, respectively. These values change to 3.8 Å and 4.9 Å, respectively, with a ten-fold increase in the negative ion polarizabilities. There is an alternative energy transfer mechanism to describe quenching by $CO_2$. The $CO_2$ $A^1B_2$ state lies just above the ground vibrational state of NO $A^2\Sigma^+$ which could lead to a near-resonant $E \rightarrow E$ transfer mechanism. Emission from the $A \leftrightarrow X$ system of $CO_2$ is observed in the range of 310 nm to 380 nm while the system is seen in absorption from 140 nm to 175 nm. This suggests that the near-resonant interaction is weakly allowed from a $|\langle CO_2|CO_2^*\rangle|$ Franck-Condon standpoint.

The prediction of the full model, using the parameters listed in Table 1 and a value of $P_R = 0.6$, are shown in Figs. 4 and 5 for $CO_2$ and $H_2O$, respectively. Also given are several sets of measured quenching cross-sections. For $CO_2$ and $H_2O$ at elevated temperatures, the model predicts a relatively constant cross-section with temperature. The increased cross-section predicted at room temperature is a direct result of including the action of a collision complex. The present model appears to capture much of the behavior measured for $H_2O$ and for $CO_2$. In our early application of this model we employed a value of 0.35 D for the dipole moment of NO $A^2\Sigma^+$ ($v' = 0$). Using this value and a thermally averaged attractive potential the model noticably underpredicted the cross-section for $CO_2$ at low temperatures. Re-evaluation of the works of Langhoff et al. [47] and Bergman and Zare [48] suggests a value of order 1.1 D for NO $A^2\Sigma^+$ ($v' \leq 3$). This higher value, employed in the present work, leads to a noticable improvement in the predictive capibility of the model, particularly for

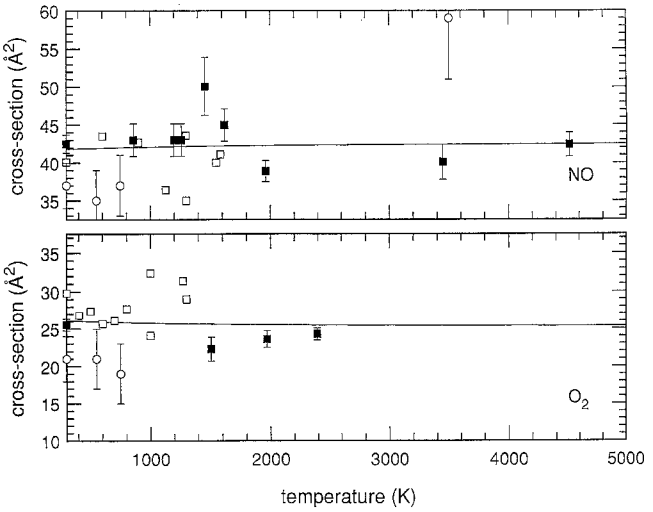


**Fig. 3.** Cross-section for quenching of NO $A^2\Sigma^+$ ($v' = 0$) by NO and $O_2$. *Solid line*: full model prediction for a thermal distribution vibrationally excited collision partners. Measured values: ■ [10, 12], ○ [8, 9], □ [6]

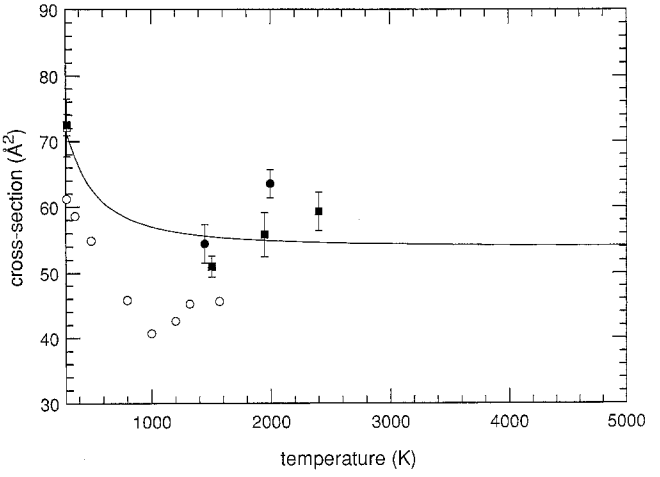


**Fig. 4.** Cross-section for quenching of NO $A^2\Sigma^+$ ($v' = 0$)by $CO_2$. *Solid line*: full model prediction. Measured values: ■ [12], • [10], ○ [6], □ [16]

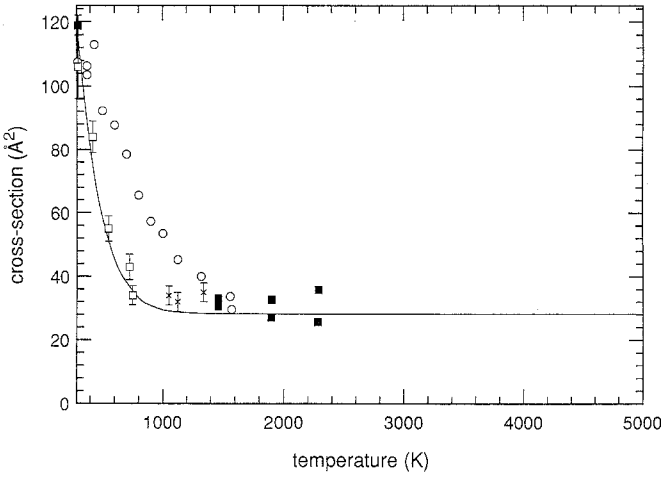


**Fig. 5.** Cross-section for quenching of NO $A^2\Sigma^+$ ($v' = 0$) by $H_2O$. *Solid line*: model prediction. Measured values: ■ [12], ○ [6], □ [8], × [7]

interactions with $CO_2$ and $H_2O$. The $N_2O$ and $CO_2$ negative ions are quite similar [45] thus $N_2O$ and $CO_2$ are predicted to have very similar quenching cross-section behavior. For quenching of NO $A^2\Sigma^+$ ($v' = 0$) by $N_2O$, Greenblatt and Ravishankara [16] report a value of 64.1 Å$^2$ at 300 K while shock tube measurements [12] give values of 80 Å$^2$ at 300 K and 60 Å$^2$ at 1450 K and 2300 K, confirming this prediction.

The measured cross-section for quenching of NO $A^2\Sigma^+$ ($v' = 0$) by $SO_2$ noticeably exceeds that predicted by the simple harpoon model (even though $SO_2$ displays a relatively large positive affinity). Asscher and Haas [18] have suggested that this may be the result of near-resonant energy transfer with the $SO_2$ $\tilde{A}^1A_2$ state. Although they have noted [43] that in the experiments $SO_2$ fluorescence was not observed subsequent to NO excitation. Failure to observe induced $SO_2$ fluorescence is likely to be the result of $SO_2$ self-quenching or quenching by the NO and the bath gas (e.g. for $SO_2$ $\tilde{A}^1A_2$ the measured quenching cross-sections are of order: 33, 99 124, 117, and 484 Å$^2$ for He, Ar, $N_2$, NO, and $SO_2$, respectively [14]). Thus the near-resonant process cannot be wholly ruled out. However, the use of the combined harpoon/collision-complex model is indicated, particularly in light of the large $SO_2$ dipole moment and the fact that electron transfer to the ground-state negative ion is reasonably Franck-Condon allowed [45]. Using the full model and a value of $P_R = 0$, the predicted cross-section is 136 Å$^2$ at 300 K which is in excellent agreement with the measured value of 140 Å$^2$. The prediction shows a high-temperature limiting value of 62 Å$^2$, which appears to be reasonably constant for temperatures over 900 K.

For polyatomic colliders with large affinities we have suggested that the cross-section should fall in the range of $\pi b_Z^2 < \sigma < \pi r_c^2$. A cross-section for $CCl_4$ based on $b_Z$ is two times smaller than the value measured by Asscher and Haas [18], however, the larger value reported by Haas and Greenblatt [19] is consistent with a prediction based upon $r_c$. For quenching NO $A^2\Sigma^+$ ($v' = 0$) by $NO_2$, Haas and Greenblatt [19] report a quenching cross-section of 46 Å$^2$ at 300 K and Thoman et al. [12] report values of 90 Å$^2$ at 300 K and 1450 K, and 85 Å$^2$ at 1900 K. We find $r_c \cong 10.5$ Å

**Table 3.** Potential near-resonant collision partners

| | State | Energy [cm$^{-1}$] | $E_{fM}$ [eV] | $\mu$ [D] | $\sigma_Q$ [Å$^2$] | $\sigma_g$ [e] [Å$^2$] | $\sigma_0$ [f] [Å$^2$] | Note |
|---|---|---|---|---|---|---|---|---|
| NO | $A^1\Sigma^+$ | 44200 | 0.024 | 0.157 | 42.7[c] | | | for ref. |
| $CO_2$ | $A^1B_2$ | 46000 | −0.2 | 0.0 | 74.0[c] | g | g | a |
| $C_6H_6$ | $a^3B_{1u}$ | 29510 | −1.1 | 0.0 | 116.0[d] | g | g | b |
| | $A^1B_{2u}$ | 38086 | | | | | | |
| $NO_2$ | $A^2B_1$ | <15000 | 2.4 | 0.32 | 90.0[c] | 344.2 | 42.3 | |
| | $B^2B_2$ | 40126 | | | 46.0[d] | | | |
| $N_2O$ | $a^3\Pi$ | 32630 | 0.24 | 0.16 | 80.0[c] | g | g | |
| | $b^3\Pi$ | 35460 | | | 63.5[d] | | | |
| | $A^1\Sigma^+$ | 38500 | | | | | | |
| $O_3$ | $A$ | 10000 | 2.103 | 0.53 | na | 236.9 | 44.8 | |
| | $B$ | 16625 | | | | | | |
| | $C$ | 23447 | | | | | | |
| | $D$ | 33000 | | | | | | |
| $SO_2$ | $a^3B_1$ | 25767 | 1.06 | 1.633 | 140.0[d] | 97.5 | 58.4 | b |
| | $A^1B_1$ | 29622 | | | | | | |
| | $C$ | 41431 | | | | | | |
| | $D$ | 42264 | | | | | | |
| Biacetyl | $B^1A_u$ | 35500 | 0.63 | 1.78 | na | 85.0 | 68.6 | |
| | $A^1A_u$ | 21983 | | | | | | |
| $CF_3I$ | $A$ | 35500 | 1.4 | ≈0.0 | 132.0[d] | g | g | b |
| $CH_3I$ | $A$ | 28000 | 0.2 | 1.62 | 160.0[d] | 78.0 | 90.0 | b |

[a] $|\langle M \mid M^* \rangle|$ array does not support a near-resonant mechanism
[b] $E \rightarrow E$ resonant or resonant/harpoon behavior suggested [18, 19]
[c] measured 300 K [12]
[d] measured 300 K [16, 18, 19, 43]
[e] predicted harpoon maximum
[f] predicted harpoon minimum
g full model required for prediction
na not available

and $b_Z \cong 3.7$ Å giving cross-sections of 344 Å$^2$ and 42 Å$^2$, respectively. A full model calculation was performed for quenching by $NO_2$. The acceptor Franck-Condon array was generated using a harmonic approximation with the structural constants and the value for the $\langle 0,0,0|0,0,0\rangle$ element obtained from photodetachment measurements [49, 50]. The predicted behavior is consistent with the view that the high-temperature limit for quenching by $NO_2$ is functionally established by 400 K. Above this temperature the cross-section is predicted to be near constant with a value of 64.5 Å$^2$. The magnitude of the prediction is within the range of the measurements (which vary by a factor of two at 300 K), and is consistent with the observed temperature dependence.

Table 3 gives the predicted room-temperature cross-sections, based on $b_Z$ and $r_c$, for a number of polyatomic quenching partners as compared to the available experimental data. An important observation is that many of these species also display large dipole moments, thus a centripetal barrier may be important at lower temperatures. Further, a number of the species listed in this Table 3 may exhibit "near-resonant enhanced" quenching. Also given in Table 3 are: the term energies for the near-resonant candidate states, the electron affinities, the dipole moments for the ground states, and, for reference, the same parameters for NO. Many molecular species that are useful as diagnostic tracers fall into this category. This suggests that combined use of NO fluorescence with Raman scattering from halocarbons or fluorescence from biacetyl, say, should be carefully tested for quenching interactions. In this regard, certainly any collision partner that has a strongly allowed electronic transition at energies less than that of the NO $A^2\Sigma^+$ should be suspect.

Quenching by radicals, negative ions and atomic species is an important question in applications to reaction flows. Cross-sections for such species are often unknown and many of these species are relatively light and as such can contribute a noticeable quenching rate even when present in moderate concentrations. Using the parameters given in Table 1 the value for the outer crossing radii for H, O, CH, OH, and NH are found to be 5.27, 6.24, 5.68, 7.33, and 4.31 Å, respectively. The value for NH would increase to 4.44 Å given a three-fold increase in the negative ion polarizability. These values are expected to be relatively temperature insensitive, particularly for H, O and OH, the later having a highly diagonal acceptor Franck-Condon array [50, 51]. Even though the crossings for these species occur at large radii, the unit weighting for the electronacceptor serves to maintain a large value for $v_{LZ}$. However, the present indication from our shock-tube measurements is that quenching by O and H proceed with a substantially smaller cross-section than predicted at elevated temperatures. One possible explanation for the discrepancy may be found in the assumption of an angle-independent electronic matrix element. The use of a $\cos^2\theta$ distribution in the definition for $h'_{12}$ reduces the predicted O quenching cross-section to 57 Å$^2$ from a value of 122 Å$^2$ obtained from the angle-independent simulation [27].

## 4 Conclusions

We have evaluated a "harpoon" or "curve-crossing" model to describe quenching of NO $A^2\Sigma^+$ by a wide variety of collision partners which are of interest in combustion and aerothermodynamic applications. The model is found to be quite successful predicting both the magnitude and the temperature dependence of the quenching cross-section when combined with the action of a "collision-complex". For situations where the crossing is reasonably allowed, the basic character of the solution is strongly attractive and yields a nearly temperature-independent solution. For slightly negative electronic affinities, weakly allowed outer crossings, and for crossing on an energy barrier the effect of secondary mechanisms, collision-complex formation or near-resonant energy transfer, say, are found to be quite important. In the present model, the mechanics of transfer through the NO $X^2\Pi$ exit channel have been relegated to a simple multiplicative constant. However, the implied mechanism suggest that quenching produces vibrationally excited NO $X^2\Pi$, which appears to be in accord with the experimental observations.

We note that the present model captures the temperature dependence but overpredicts the magnitude of the quenching cross-section for the simplest collision partners (e.g. atomics and homonuclear diatomics). These species should pose the simplest orientation dependence in the electronic matrix element and as such are most likely to violate the isotropic assumption. For these simple species this suggests that when the entrance channel is accessible, some degree of reorientation is required to make the exit channel also accessible. Such an adjustment would be unlikely on the transfer timescales. Thus $(1 - P_R)$ may be significantly less than unity and to a reasonable approximation may be taken as a constant (e.g. the value of the angular overlap integral of the product of the electron transfer probabilities for the entrance and exit channels).

This is a phenomenological model and as such it is useful to estimate bounds for unknown cross-sections to extrapolate experimental data beyond the measurement temperature range, of to evaluate cross-sections for excited vibrational states. Further developments to the model must involve a more detailed description of the orientation dependence of the electronic matrix element as well as a more substantial data base on the variation of molecular (neutral, excited and ion) electronic properties with vibrational level.

*Acknowledgements.* This research was supported by the United States Department of Energy, Office of Basic Energy Sciences, Chemical Sciences Division. JWT acknowledges the support of Associated Western Universities for an AWU-DOE faculty sabbatical fellowship.

## References

1. P.H. Paul, M.P. Lee, R.K. Hanson: Opt. Lett. **14**, 417 (1989)
   J.M. Seitzman, G. Kychakoff, R.K. Hanson: Opt. Lett. **10**, 439 (1985)
   B.K. McMillin, M.P. Lee, R.K. Hanson: AIAA J. **30**, 436 (1991)
2. R.S. Barlow, R.W. Dibble, J.Y. Chen, R.P. Lucht: Combust. Flame **82**, 235 (1990)
   R.W. Pitz, J.A. Wehrmeyer, J.M. Bowling, T.S. Cheng: Appl. Opt. **29**, 2325 (1990)
3. G. Zizak, F. Cignoli, S. Benecchi: Appl. Phys. B **51**, 67 (1990)
4. H. Zacharias, J.B. Halpern, K.H. Welge: Chem. Phys. Lett. **43**, 41 (1976)

5. I.S. McDermid, J.B. Laudenslanger: J. Quant. Spectrosc. Radiat. Transfer **27**, 483 (1982)
6. M.C. Drake, J.W. Ratcliffe: High temperature quenching cross sections for nitric oxide laser-induced fluorescence measurements. (General Motors Research Laboratories, Report GMR-7426 1991)
7. R.J. Cattolica, T.G. Mataga, J.A. Cavolowsky: J. Quant. Spectrosc. Radiat. Transfer **42**, 499 (1989)
8. G.A. Raiche, D.R. Crosley: J. Chem. Phys. **92**, 5211 (1990)
9. U.E. Meier, G.A. Raiche, D.R. Crosley, G.P. Smith, D.J. Eckstrom: Appl. Phys. B. **53**, 138 (1991)
10. J.A., Gray, P.H. Paul, J.L. Durant: Chem. Phys. Lett. **190**, 266 (1992)
11. J.W. Thoman Jr., J.A. Gray, J.L. Durant Jr., P.H. Paul: Collisional electronic quenching of NO $A^2\Sigma^+$ by $N_2$ from 300 to 4500 K. J. Chem. Phys. **97**, 8156 (1992)
12. J.W. Thoman Jr., J.A. Gray, J.L. Durant Jr., P.H. Paul: Collisional electronic quenching of NO $A^2\Sigma^+$ by $H_2O$, $O_2$, CO, $CO_2$, NO, $NO_2$, $N_2O$, $N_2$, $CH_4$, $H_2$ and Ar. J. Chem. Phys. (1992) to be published
13. D. R. Crosley: personal communication SRI (1991)
14. D.L. Holterman, E.K.C. Lee, R. Nanes: J. Chem. Phys. **77**, 5327 (1982)
15. W. Fairchild, G.P. Smith, D.R. Crosley: J. Chem. Phys. **79**, 1795 (1983)
16. D.G. Greenblatt, A.R. Ravishankara: Chem. Phys. Lett. **136**, 501 (1987)
17. C.S. Parmenter, M. Seaver: Chem. Phys. Lett. **67**, 279 (1979)
18. M. Asscher, Y. Haas: J. Chem. Phys. **76**, 2115 (1982)
19. Y. Haas, G.D. Greenblatt: J. Phys. Chem. **90**, 513 (1986)
20. B.M. Smirnov: *Negative Ions* (McGraw-Hill, New York 1982)
21. E. Bauer, E.R. Fisher, F.R. Gilmore: J. Chem. Phys. **51**, 4173 (1969)
22. J.T. Yardley: *Introduction to Molecular Energy Transfer* (Academic, New York 1980)
23. H. Margenau, N.R. Kester: *Theory of Intermolecular Forces* (Pergamon, Oxford 1969)
24. J.O. Hirschfelder, C.F. Curtiss, R.B. Bird: *Molecular Theory of Gases and Liquids* (Wiley, New York 1964)
25. H.E. Revercomb, E.A. Mason: Anal. Chem. **47**, 970 (1975)
26. N.F. Mott, H.S.W. Massey: *Atomic Collisions* (Oxford University Press, Oxford 1965)
27. E.A. Gislason, J.G. Sachs: J. Chem. Phys. **62**, 2678 (1975)
28. E.R. Fisher, G.K. Smith: Appl. Opt. **10**, 1803 (1971)
29. J.B. Hasted, A.Y.J. Chong: Proc. Phys. Soc. **80**, 441 (1962)
30. R.E. Olsen, F.T. Smith, E. Bauer: Appl. Opt. **10**, 1848 (1971)
31. T. Su, M.T. Bowers: Classical ion-molecule collision theory, in *Gas Phase Ion Chemistry I*, ed. by M.T. Bowers (Academic, New York 1979)
32. E.A. Gislason: J. Chem. Phys. **58**, 3702 (1973)
33. for NO: M. W. Seigel, R.J. Celotta, J.L. Hall, J. Levine, R.A. Bennet: Phys. Rev. A **6**, 607 (1972)
    R.J. Celotta, R.A. Bennet, J.L. Hall, M.W. Seigel, J. Levine: Phys. Rev. A **6**, 631 (1972)
    for $O_2$: M.J. Travers, D.C. Cowles, G.B. Ellison: Chem. Phys. Lett. **164**, 449 (1989)
34. E.A. Mason, E.W. McDaniel: *Transport Properties of Ions in Gases* (Wiley, New York 1988)
    E.W. McDaniel, E.A. Mason: *The Mobility and Diffusion of Ions in Gases* (Wiley, New York 1973)
35. A.A. Radzig, S.M. Smirnov: *Reference Data on Atoms, Molecules and Ions*, Springer Ser. Chem. Phys., Vol. 31 (Springer, Berlin, Heidelberg 1985)
36. K.P. Huber, G. Herzberg: *Constants of Diatomic Molecules* (Van Nostrand, New York, 1979)
37. A. Lofthus, P.H. Krupenic: Phys. Chem. **6**, 113 (1977)
38. T. Imajo, K. Shibuya, K. Obi, I. Tannaka: J. Phys. Chem. **90**, 6006 (1986)
39. H.P. Broida, T. Carrington: J. Chem. Phys. **38**, 136 (1963)
    A.B. Callear, M.J. Pilling: Trans. Faraday Soc. **66**, 1618 (1970)
40. T.G. Slanger, G. Black: J. Chem. Phys. **60**, 468 (1974)
41. G. Karl, P. Kruus, J.C. Polanyi: J. Chem. Phys. **46**, 224 (1967)
42. W.H. Breckenridge, R.P. Blickensderfer, J. Fitzpatrick, D. Oba: J. Chem Phys. **70**, 4751 (1979)
43. Y.A. Haas, M. Asscher: Two-photon excitation as a kinetic tool: applications to nitric oxide fluorescence quenching, in *Adv. in Chemical Physics XLVII: Photoselective Chemistry II*, ed. by J. Jortner, R.D. Levine, S.A. Rice (Wiley, New York 1981)
44. V.I. Vedeneyev, L.V. Gurich, V.N. Kondrat'yev, V.A. Medvedev, Ye.L. Frankevich: *Bond Energies Ionization Potentials and Electron Affinities* (Edward Arnold, London 1962)
45. H.S.W. Massey: *Negative Ions* (Cambridge University Press, Cambridge 1976)
46. S.Y. Tang, E.W. Rothe, G.P. Reck: J. Chem. Phys. **61**, 2592 (1974)
    Y. Yoshioka, H.F. Schaefar, K.D. Jordan: J. Chem. Phys. **75**, 1040 (1981)
    W.B. England: Chem. Phys. Lett. **78**, 607 (1981)
47. S.R. Langhoff, C.W., Bauschilicher, H. Partridge: J. Chem. Phys. **89**, 4909 (1988)
48. T. Bergman, R.N. Zare: J. Chem. Phys. **61**, 4500 (1974)
49. S.B. Woo, E.M. Helmy, P.H. Mauk, A.P. Paszek: Phys. Rev. A **24**, 1380 (1981)
50. R.J. Cellota, R.A. Bennet, J.L. Hall: J. Chem. Phys. **60**, 1740 (1974)
51. P.A. Schulz, R.D. Mead, P.L. Jones, W.C. Lineberger: J. Chem. Phys. **77**, 1153 (1982)
52. B.K. Janousek, J.I. Brauman: Electron affinities, in *Gas Phase Ion Chemistry II*, ed. by M.T. Bowers (Academic, New York 1979)
    P.S. Drzaic, J. Marks, J.I. Brauman: Electron photodetachment for gas phase molecular anions, in *Gas Phase Ion Chemistry III*, ed. by M.T. Bowers (Academic, New York 1984)
53. J. Applequist, J.R. Karl, K.-K. Fung: J. Am. Chem. Soc. **94**, 2953 (1972)
54. P.E. Cade: J. Phys. Chem. **47**, 4649 (1967)
55. G.J. Schulz: Phys. Rev. A **135**, 988 (1964)
56. A. Kayar, J. Bonamy: J. Quant. Spectrosc. Radiat. Transfer **28**, 45 (1982)